On the Relevance of Node Isolation to the K-Connectivity of Wireless Optical Sensor Networks

Unoma Ndili Okorafor, *Member*, *IEEE*, and Deepa Kundur, *Senior Member*, *IEEE*

Abstract—In designing wireless multihop sensor networks, determining system parameters that guarantee a reasonably connected network is crucial. In this paper, we investigate node isolation in wireless optical sensor networks (WOSNs) as a topology attribute for network connectivity. Our results pertain to WOSNs modeled as random-scaled sector graphs that employ directional broad-beamed free space optics for point-to-point communication. We derive a generalized analytical expression relating the probability that no node is isolated to the physical layer parameters of node density, transmitter radius, and angular beam width. Through simulations, we demonstrate that for probability values close to 1, dense networks, and increasing beam width, the probability that the WOSN is connected is tightly upper bounded by the probability that no isolated node exists. In addition, our study demonstrates conditions for probabilistic K-connectivity guarantees and provides empirical insights on the impact of clustering on connectivity by employing simulations to validate analytical derivations. Our analysis provides a methodology of practical importance to choosing physical layer parameter values for effective network level design.

Index Terms—Wireless optical sensor networks, node isolation, K-connectivity, hierarchical random-scaled sector graph.

1 Introduction

The need for untethered communications and computing continues to drive advances in mobile communications and wireless networking. To serve this purpose, *wireless sensor networks* (WSNs) have been envisioned to consist of groups of lightweight sensor nodes that may be randomly and densely deployed to observe data within a physical region of interest. The nodes form an ad hoc multihop network, communicating their sensor readings to a *base station*. The connectivity of these self-organizing WSN systems is critical for reliable sensing and inference capabilities [1].

Conventionally, sensor network research has focused on nodes that transmit (and receive) data via omniangle radio frequency (RF) technology. Modeled as a *geometric random graph* (GRG), two nodes s_i and s_j establish a bidirectional link or edge denoted as $s_i \leftrightarrows s_j$, if they are within a fixed placement distance r (known as *communication radius*) [2]. Recently, however, there has been increased interest in the development of *wireless optical sensor networks* (WOSNs) [3], [4], [5], [6] composed of nodes whose point-to-point communication paradigm employs directed broad-beam free space optics (FSO); WOSNs transmit by scanning a directional line-of-sight (LOS) laser beam over a "pie-shaped" angular sector. WOSNs have recently been modeled as a *random-scaled sector graph* (RSSG) [7]. Here, a *directed* link or edge denoted as $s_i \rightarrow s_j$ is established from node s_i to s_j if and only if s_j falls within s_i's communication sector. A path from s_j to s_i may likely consist of a multihop reverse back channel denoted as $s_j \rightsquigarrow s_i$, which employs a sequence of other nodes acting as routers.

Interest in WOSNs is motivated, in part, by increased spatial reuse for communications, smaller node size, ultrahigh bandwidths, and reduction in interference and expended energy for the same transmission radius (thus increasing network lifetime and throughput). Furthermore, security is enhanced due to the reduced spatial signature for communications making eavesdropping more difficult. One of their biggest challenges, however, involves establishing network connectivity especially for random deployments. While solutions have been proffered for random RF WSN connectivity, to the best of our knowledge, the corresponding problem for WOSNs has not been previously addressed. This paper seeks to address the WOSN connectivity problem, and present analytic results that yield constraints on physical layer parameters of WOSN nodes such that probabilistic connectedness of the network is guaranteed.

1.1 Ad Hoc Network Connectivity and Node Isolation

Connectivity is often viewed as a metric for the robustness, survivability, or fault tolerance of networks, and has also been related to the value of a network [8]. Traditionally, a network is said to be *connected* if, for every possible node pair, there exists at least one path (sequence of nodes and edges) connecting them. For a directed network, which is composed of directed edges, a *strongly connected* network is one in which, for every node pair (s_a, s_b), both paths $s_a \rightsquigarrow s_b$

- *U.N. Okorafor is with Texas Instruments, 7800 Banner Drive, Dallas, TX 75251. E-mail: unomao@gmail.com.*
- *D. Kundur is with the Department of Electrical and Computer Engineering, Texas A&M University, 111D Zachry Engineering Center, 3128 TAMU, College Station, TX 77843-3128. E-mail: deepa@ece.tamu.edu.*

Manuscript received 27 Feb. 2008; revised 8 Dec. 2008; accepted 10 Feb. 2009; published online 10 Mar. 2009.
For information on obtaining reprints of this article, please send e-mail to: tmc@computer.org, and reference IEEECS Log Number TMC-2008-02-0063. Digital Object Identifier no. 10.1109/TMC.2009.57.

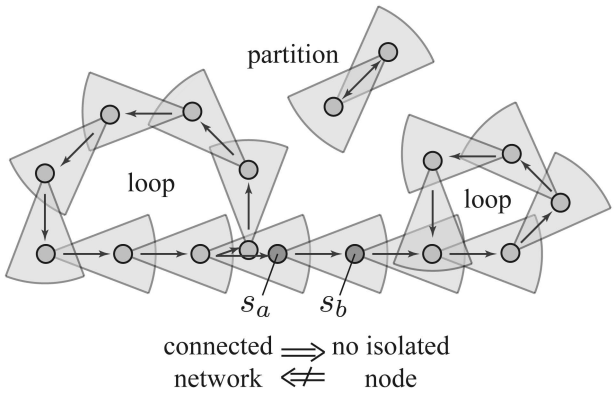

Fig. 1. The WOSN has no isolated nodes since every node has both an incoming and an outgoing link. However, the overall network is not (strongly) connected due to the network partition and link directionality.

and $s_b \rightsquigarrow s_a$ exist [9]. In this paper, unless ambiguous, we shall refer to the "strongly connected" property of WOSNs simply as "connected."

For randomly deployed ad hoc networks, an exact closed-form expression relating physical layer parameters to the degree of connectivity remains an open problem. A more tractable approach relates the conditions under which there is no isolated network node to network connectivity; this has been studied for RF WSNs [10], [11], but not directional networks. Obviously, the occurrence of isolated nodes undermines the goal of achieving a connected network; the existence of even a single isolated node implies that the network is necessarily disconnected. Thus, a connected network implies that there are no isolated nodes; however, the converse is not true. Fig. 1 demonstrates how for WOSNs even though there are no isolated nodes, the network is not connected due to link directionality and partitions; for example, $s_b \rightsquigarrow s_a$ does not exist, even though $s_a \rightarrow s_b$ exists, and nodes in the partition cannot communicate to other nodes in the network. Therefore, guaranteeing that no isolated node exists provides only a necessary condition for connectivity albeit it is an important starting point.

Recently, it was demonstrated for RF WSNs that the probability that no isolated node occurs is a *tight upper bound* for the probability that the network is connected as the number of nodes $n \rightarrow \infty$ and for probabilities close to 1 [10], [11]. This result further motivates our study of network conditions and parameters that ensure a "no isolated node" property, and its relevance to network connectivity for WOSNs. One issue we address in this paper is whether the results of [10] for RF WSNs also apply to the WOSN network model.

1.2 Contributions

We employ probabilistic methods to address the *parameter assignment problem* for a WOSN. We study how the number of nodes n, communication radius r, and communication laser beam width α should be selected to guarantee with high probability that there is no isolated WOSN node, and how the results relate to actual connectivity. First, we introduce the notion of two distinct neighborhoods for each WOSN node facilitating the derivation of an analytical expression for the probability p_d that no isolated node occurs as a function of n, r, and α. Second, we compare our analytic expressions with empirical results to demonstrate that similar properties presented in [10] for omnidirectional RF WSNs also hold for WOSNs as $\alpha \rightarrow 2\pi$. Third, we analyze the impact of hierarchy on WOSN connectivity as a function of the fraction of cluster head nodes to empirically show that clustering improves connectivity. The WOSN analysis also relates, in part, to emerging hybrid RF/FSO and directional RF networks [12]; thus, our discussion of connectivity for WOSNs also serves as a first step to the analysis of such emerging ad hoc networks.

The next section presents related work, while Section 3 introduces the WOSN network model. Section 4 presents a probabilistic analysis and simulations for the WOSN node isolation property. Section 5 provides insights into the probability of connectivity for the WOSN and its relation to node isolation, and explores the impacts of clustering on hierarchical connectivity. Concluding remarks are presented in Section 6.

2 WSN Connectivity

In general, a connected network is desirable for optimal functioning of mechanisms such as neighborhood discovery, routing, and clustering. Equally important for network performance are issues involving energy constraints and shared communication medium. For this reason, connectivity analysis often involves identifying minimum values for communication range r and/or number of nodes n that guarantee a connected network. Minimizing r effectively minimizes the energy expended by each node for communications optimizing network lifetime, while minimizing n reduces interference from neighboring nodes optimizing throughput.

Formally, this analysis is related to the *range assignment problem* defined as follows for RF WSNs: *given a set of n nodes randomly deployed in a geographical region of fixed area, all having the same r, what is the minimum value of r that ensures the resulting GRG network is connected?* The solution is crucial for defining WSN design guidelines that minimize cost answering questions as to the type of transceiver that should be employed in each node (classified by the value of parameters such as r) and the number of nodes that should be dispersed. Other generalized variants of the problem (in which the transmission range is different for each node) exist that are shown to be NP-hard, but we do not consider them.

One approach to the RF WSN range assignment problem applies *asymptotic* reasoning to provide connectivity assurances as the region size or n grows to infinity. In a pioneering paper on the critical node transmit power to ensure a connected network, Gupta and Kumar [2] employ results from continuum percolation theory and random graphs to derive a sufficient condition on r as a function of n. They show that for n nodes uniformly deployed in a planar unit area disk, if $r \geq \sqrt{\frac{\log(n)+c(n)}{\pi n}}$, then the GRG network is asymptotically almost surely (a.a.s.) connected (as $n \rightarrow \infty$ with probability 1), only if $\lim_{n\rightarrow\infty} c(n) = +\infty$, where $c(n)$ is a constant. In [13], Santi and Blough present related

connectivity results for sparse networks by introducing a geometric parameter that bounds the deployment area.

Other papers have analyzed asymptotic connectivity of the GRG with respect to the minimum number of neighbors required by each node in a k-neighbor model. In [14], Kleinrock and Silvester optimize an objective throughput function based on the average number of neighbors, and suggest that a fixed *magic* number of neighbors equal to *six* is sufficient to guarantee network connectivity, regardless of the value of n. Takagi and Kleinrock [15] later revised this magic number to *eight*. In [16], Xue and Kumar show that there is no magic number, but rather that the number of neighbors required grows as $\Theta(\log n)$. In particular, they show that this number must be larger than $0.074 \log n$ and less than $5.1774 \log n$. In [17], the authors show an improved lower bound for the number of neighbors of $0.129 \log n$.

More generally, Penrose studied k-connectivity of GRG networks deployed in d-dimensional cubes for $d \geq 2$ [18]. He proved that for $n \to \infty$, the minimal r for which the graph is almost surely k-connected is equal to the minimum r that ensures with probability one that each node has at least k neighbors. Thus, to guarantee connectivity in dense networks, it suffices to adjust r until each node has at least one neighbor (i.e., no isolated node exists in the network).

Employing a *probabilistic* approach and nearest k-neighbor methods, Bettstetter [10] showed that for a ρ-density network, no isolated node occurs with probability at least p if $r \geq \sqrt{\frac{-\ln(1-p^{1/n})}{\rho\pi}}$. Leveraging the results of [18] and assuming that boundary conditions are compensated for, he empirically demonstrates that for nodes deployed in a bounded region, $n \to \infty$ and $p \to 1$, the probability that no isolated node occurs yields a tight upper bound on the probability that the network is connected. A related analysis of range assignment in the presence of fading links has also been considered [19].

While prior art provides insightful results, most research pertains to omnidirectional RF WSNs modeled as GRGs with the exception in [7] that considers WOSNs. In [7], Diaz et al. employ asymptotic arguments ($n \to \infty$) to show that for the same constraint on r as obtained in [2], with high probability, any edge in the undirected GRG associated to a WOSN may be emulated by a path of length at most four in the directed RSSG induced by the WOSN. They also provide asymptotic bounds on the expected maximum and minimum in and out degree of nodes to achieve a connected WOSN. While of great theoretic interest, the results lack real-world applicability in WSN scenarios involving finite-area deployment regions and number of nodes. For this reason, we consider a probabilistic approach to network connectivity and the parameter assignment problem in dense WOSNs.

Our novel analysis follows the probabilistic flavor of [10], but applied to the RSSG model pertaining to WOSNs. We also, for the first time, investigate the relevance of node isolation to network connectivity as in [18], but in regard to WOSNs. Additionally, we consider the effects of hierarchy and clustering on the connectivity of heterogeneous WOSNs that include a sparse subnetwork of randomly placed FSO cluster heads. We expect that our results will impact practical neighborhood discovery and routing algorithms for emerging WOSNs [20], [21].

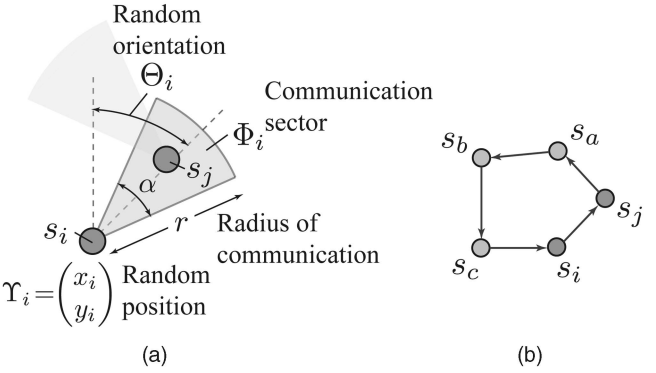

Fig. 2. (a) Each WOSN node s_i transmits within a sector Φ_i defined by the 4-tuple $(\Upsilon_i, \Theta_i, r, \alpha)$. (b) Node s_j can only hear node s_i as it falls into s_i's communication sector; however, s_j transmits to s_i via the back channel $s_j \to s_a \to s_b \to s_c \to s_i$.

3 Directional Sensor Network Model

Consider a set $\mathcal{S}_n = \{s_i : i = 1, 2, \cdots n\}$ of n WOSN nodes, randomly and densely deployed in a bounded, unit area, planar square region $\mathcal{A} = [0, 1]^2$ according to a uniform distribution. Each sensor has an equal and independent likelihood of falling at any location in $\mathcal{A}$, and facing any orientation. Let vectors $\overline{x} = (x_1, x_2, \cdots x_n)$ and $\overline{y} = (y_1, y_2, \cdots y_n)$ represent the (x, y) position coordinates of $\mathcal{S}_n$ such that $(x_i, y_i) \sim \text{Uniform}(0, 1)^2$. For ease of reference, let $\Upsilon_i = \binom{x_i}{y_i}$ be s_i's point position, where $\overline{\Upsilon} = \binom{\overline{x}}{\overline{y}}$. The vector $\overline{\Theta} = (\Theta_1, \Theta_2, \cdots \Theta_n)$ depicts the random orientations associated with $\mathcal{S}_n$ such that $\Theta_i \sim \text{Uniform}[0, 2\pi), \forall s_i \in \mathcal{S}_n$. The spatial distribution of the nodes is modeled as a homogenous Poisson point process [22], [23] of density $\frac{n}{|A|}$, where $|A|$ is the area of $\mathcal{A}$, which is unity in our case, making n the network density of our deployment region.

Directional optical sensor nodes employ a directed broad-beam FSO transmitter suitable for short-range networking applications [24]. By scanning a laser beam across an angular sector, each node s_i can send data within a contiguous, randomly oriented communication sector $-\frac{\alpha}{2} + \Theta_i \leq \Phi_i \leq +\frac{\alpha}{2} + \Theta_i$ of radius r and angle $\alpha \in [0, 2\pi)$ radians, as depicted in Fig. 2a, where Θ_i is the orientation of s_i. The communication sector Φ_i which is completely defined by the 4-tuple $(\Upsilon_i, \Theta_i, r, \alpha)$ is associated with node s_i. The node's receiver is omnidirectional (employing several photodetectors [24]) implying that s_i may directly talk to s_j (denoted as $s_i \to s_j$) if and only if $\Upsilon_j \in \Phi_i$. However, s_j can only talk to s_i via a multihop back channel or reverse route, with other nodes in the network acting as routers along the reverse path, unless, of course, $\Upsilon_i \in \Phi_j$. In the illustration of Fig. 2b, an example of a reverse route for $s_j \rightsquigarrow s_i : s_j \to s_a \to s_b \to s_c \to s_i$ is shown. Naturally, in discovering a multihop-directed reverse path, the notion of a circuit, first proposed for routing in [25], results and serves as the fundamental mechanism for bidirectional communication in WOSNs.

The random multihop WOSN cooperatively formed by $\mathcal{S}_n$ is defined by parameters n, r, and α and is modeled as an RSSG that is formally defined as follows [7]:

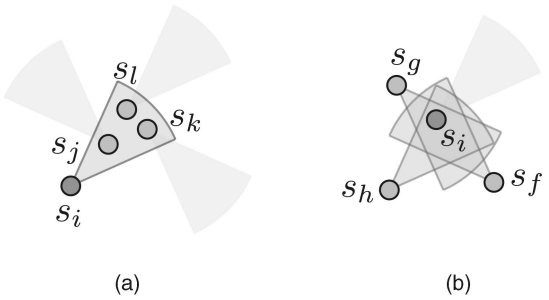

Fig. 3. Distinct neighborhoods of a WOSN node s_i. (a) Successors: s_j, s_k, s_l. (b) Predecessors: s_f, s_g, s_h.

Definition 3.1. *For any natural n, fixed angle α and range r, let $\mathcal{S}_n = \{s_i\}_{1\le i\le n}$ be a sequence of independently and uniformly distributed (i.u.d.) random vertices in $[0,1]^2$, and let $\Theta = (\Theta_i)_{1\le i\le n}$ be a sequence of i.u.d. angles in $(0, 2\pi]$ associated with $\mathcal{S}_n$. Let $\mathcal{E}$ represent the $n \times n$ adjacency matrix such that the matrix elements are assigned values: $\mathcal{E}(i,j)_{1\le i,j\le n} = 1$ if and only if $s_i \rightarrow s_j$ exists. Graph $G(\mathcal{S}_n, \mathcal{E})$ is a random-scaled sector graph.*

As common, a fraction of the WOSN nodes play the functional role of cluster heads (CHs) [26], [27], network gateways that employ advanced hardware such as passive corner cube retroreflectors (CCRs) to establish bidirectional communications with the base station. CHs can send/receive data directly to/from the base station on behalf of other nodes in their associated clusters. We mark a node s_k, which is a CH with an asterisk to give s_k^*, and denote the set of CH nodes by $\mathcal{CH}$.

3.1 Graph-Theoretic Framework

We model the n-node WOSN topology as a directed random graph $G_n(\mathcal{S}_n, \mathcal{E})$ with vertex set $\mathcal{S}_n$ and edge set $\mathcal{E}$, where every edge is an ordered pair of distinct nodes and $\mathcal{E}$ represents the $n \times n$ *adjacency matrix* [9] such that:

$$\mathcal{E}(i,j)_{1\le i,j\le n} = \begin{pmatrix} 1, & \text{if } \Upsilon_j \in \Phi_i \\ 0, & \text{otherwise} \end{pmatrix}$$

indicates that $s_i \rightarrow s_j$ exists or not, respectively, $\mathcal{E}(i,i) = 0\ \forall i$ disallows self-loops, and directionality implies $\mathcal{E}(i,j) \neq \mathcal{E}(j,i)$ necessarily, $\forall i, j$. We assume that a virtual bidirectional grid connects all CHs via the base station so that $\mathcal{E}(k,l) = \mathcal{E}(l,k) = 1, \forall s_k^*, s_l^* \in \mathcal{CH}$. In contrast to the GRG model [18], the adjacency matrix for WOSNs is sparser and nonsymmetric.

The directional paradigm necessitates that two distinct sets of neighbors be defined for each WOSN node: *successors* and *predecessors*. This distinction is significant to the connectivity analysis of WOSNs since a given node's successor may not necessarily be its predecessor (see Fig. 3), and the probability that a node's successor is also its predecessor depends on the value of α, with direct implications on the connectivity of the WOSN. The set $\mathcal{S}_i$ of s_i's *successors* is defined as: $\mathcal{S}_i =: \{s_k\}, \forall k : \mathcal{E}(i,k) = 1$, and consists of nodes that fall within Φ_i such that s_i can transmit data to such nodes. The cardinality of $\mathcal{S}_i$ is equivalent to s_i's *out degree*. Similarly, the set $\mathcal{P}_i$ of s_i's *predecessors* is defined as $\mathcal{P}_i =: \{s_h\}, \forall h : \mathcal{E}(h,i) = 1$ and consists of nodes whose communication sectors s_i fall into, so that s_i can receive data from such nodes. The cardinality of $\mathcal{P}_i$ is equivalent to s_is *in degree* [9].

Let us denote $\delta_i^+, \delta_i^- \in \mathbb{N}$ (where $\mathbb{N}$ is the set of natural numbers) as the random variables counting the number of successors and predecessors of s_i, respectively. We say that s_i is $forward_K$-*isolated* or simply f_K-*isolated* if $\delta_i^+ < K$, otherwise it is f_K-*connected*, with b_K-*isolated* and b_K-*connected* similarly defined with respect to δ_i^-. For example, s_i is f_1-isolated if $\delta_i^+ = 0$, and f_1-connected if $\delta_i^+ > 0$. A node is K-*connected* if it is both f_K-connected and b_K-connected, otherwise it is *directionally K-isolated* (i.e., either f_K-isolated, b_K-isolated, or both). In this paper, for ease of reference, 1-connected and directional 1-isolated properties are simply referred to as connected and directionally isolated, respectively. Note that our definition of a *directionally isolated* node encompasses nodes that are only partially connected (i.e., either $\delta_i^+ = 0$ or $\delta_i^- = 0$) as such nodes are undesirable in our goal of attaining a strongly connected WOSN. Where there is no risk of confusion, we refer to a directionally isolated WOSN node simply as an isolated node.

There is no K-isolated node in $G_n(\mathcal{S}_n, \mathcal{E})$ if $\forall s_i \in \mathcal{S}_n$, $\delta_i^+ \ge K$, and $\delta_i^- \ge K$. For a K-connected node, the greater the value of K, the greater its number of neighbors; Figs. 3a and 3b illustrate a node s_i that is f_3-connected and b_3-connected, respectively. A greater value of K is attractive because a network $G_n(\mathcal{S}_n, \mathcal{E})$ in which *every* node has a minimum threshold of K neighbors has a higher likelihood of multiple paths between nodes suggesting greater network redundancy for robustness to link or node failure.

4 Analysis on Node Isolation

Our first task considers the relationship between WOSN parameters when we require that no isolated node exists with probability p_d. To gain insight, we first consider the probability p_d^i that a node $s_i \in \mathcal{S}_n$ is not isolated. Let $p_f^i = \Pr[\delta_i^+ > 0]$ and $p_b^i = \Pr[\delta_i^- > 0]$ denote the probabilities that s_i is not f_1-isolated and not b_1-isolated, respectively. Recall that the set of directionally isolated nodes consists of the union of f_1-isolated and b_1-isolated nodes so that simply:

$$p_d^i = p_{f\cap b}^i = p_f^i . p_{b|f}^i, \tag{1}$$

where $\cap$ is the intersection operator, $p_{f\cap b}^i$ denotes the probability that s_i is both b_1-connected and f_1-connected (i.e., not directionally isolated), and $p_{b|f}^i$ denotes the conditional probability that s_i is b_1-connected given it is f_1-connected. Our next step then toward determining p_d^i is to evaluate p_f^i and $p_{b|f}^i$. The reader should note that we choose to conduct our analysis via conditional instead of joint probabilities because it is easier in the former setting to model the dependence between δ_i^+ and δ_i^- and its relation to α. For instance, if s_i has forward (backward) neighbors, then there is a higher likelihood that it will have one or more backward (forward) neighbors because it is known that there are nodes within the r proximity albeit they may not be at the right angle in relation to s_i. The larger the value of α, the greater the dependence/similarity between δ_i^+ and δ_i^-.

4.1 Evaluating p_f^i

Lemma 4.1. *For $n \to \infty$ and $r \ll 1$, node s_i is f_1-connected with probability p_f^i given as*

$$p_f^i = \Pr[\delta_i^+ \geq 1] = 1 - e^{\frac{-n\alpha r^2}{2}}. \tag{2}$$

Proof. We first consider the probability of the complementary event that s_i has *no* forward neighbors. The random deployment can be modeled as a Poisson distribution with a density of $n \to \infty$ and for $r \ll 1$ in the unit area region. Therefore, on average, the number of forward neighbors for node s_i is expected to be $n\frac{\alpha r^2}{2}$, where, as illustrated in Fig. 3a, $\frac{\alpha r^2}{2}$ is the pie-shaped sector area where a node must lie to be a forward neighbor of s_i. Thus, the probability that s_i is f_1-connected is: $p_f^i = \Pr[\delta_i^+ \geq 1] = 1 - \Pr[\delta_i^+ = 0] = 1 - e^{\frac{-n\alpha r^2}{2}}$. □

4.2 Evaluating p_b^i

Lemma 4.2. *For $n \to \infty$ and $r \ll 1$, node s_i is b_1-connected with probability p_b^i equal to p_f^i.*

Proof. The problem is analogous to an area coverage problem, in which s_i is "covered" if it lies within the pie-shaped communication sector of any other node as shown in Fig. 3b; s_i is b_1-connected if $\Upsilon_i \in \Phi_j$ for any $j \neq i$. Similar to the proof of area coverage derived for the general case in [28], we consider the WOSN with n nodes as points that are uniformly located in a unit area region. The probability that any point Υ_i does not fall within an arbitrary sensor's communication sector equals $(1 - \frac{\alpha r^2}{2})$, where $\frac{\alpha r^2}{2}$ is the area of the sector. Conditioned on the number of nodes n, the probability that node s_i does not lie within any node's communication sector (i.e., s_i is not covered) is $(1 - \frac{\alpha r^2}{2})^n$ [22]. For large n and $r \ll 1$, the Binomial is well approximated as a Poisson distribution so that: $\Pr[s_i \text{ is not covered}] = e^{\frac{-n\alpha r^2}{2}}$ and so: $p_b^i = 1 - e^{\frac{-n\alpha r^2}{2}}$. □

4.3 Evaluating $p_{b|f}^i$

Lemma 4.3. *For $n \to \infty$ and $r \ll 1$, node s_i is b_1-connected given it is f_1-connected with probability:*

$$p_{b|f}^i = 1 - \frac{e^{\frac{-n\alpha r^2}{2}}}{1 - e^{\frac{-n\alpha r^2}{2}}} \left(1 - \frac{\alpha r^2}{2}\right)^{n-1} \left(e^{\left[\frac{n\alpha r^2(2\pi-\alpha)}{2\pi(2-\alpha r^2)}\right]} - 1\right).$$

Proof. Assume that s_i is f_1-connected so that $\delta_i^+ \geq 1$. We evaluate $p_{b|f}^i = \Pr[\delta_i^- \geq 1 | \delta_i^+ \geq 1]$. Following our model with independently deployed nodes assumed, we consider two disjoint cases for which s_i may attain b_1-connectivity given it is already f_1-connected:

Case 1. The event that s_i has no bidirectional link with any of its successors, denoted as "no bi," implying that of the $\delta_i^+ = z$ nodes in Φ_i, none are oriented to cover s_i. In this case, s_i may only be b_1-connected if it has established a link with at least one of the $n - z - 1$ other nodes not in Φ_i, termed *nonsuccessor nodes*.

Case 2. The event that s_i has at least (a.l.) one bidirectional link with one of its successors. That is, at least one successor is also a predecessor so that s_i is b_1-connected by any of the z successor nodes in Φ_i. We refer to this event as "a.l. 1 bi,".

Due to the disjointness of Case 1 and Case 2, we have

$$\begin{aligned} p_{b|f}^i &= 1 - \Pr[\delta_i^- = 0 | \delta_i^+ \geq 1] \\ &= 1 - \big(\Pr[\delta_i^- = 0 | \delta_i^+ \geq 1, \text{no bi}] \cdot \Pr[\text{no bi}] \\ &\quad + \Pr[\delta_i^- = 0 | \delta_i^+ \geq 1, \text{a.l. 1 bi}] \cdot \Pr[\text{a.l. 1 bi}]\big). \end{aligned} \tag{3}$$

Observe that $\Pr[\delta_i^- = 0 | \delta_i^+ \geq 1, \text{a.l. 1 bi}] = 0$, as this statement is contradictory; the case that at least one bidirectional link exists cannot occur with the event that $\delta_i^- = 0$, so that the equation for $p_{b|f}^i$ simplifies to:

$$\begin{aligned} p_{b|f}^i &= 1 - \Pr[\delta_i^- = 0 | \delta_i^+ \geq 1, \text{no bi}] \cdot \Pr[\text{no bi}] \\ &= 1 - \sum_{z=1}^{n-1} \Pr[\delta_i^- = 0 | \delta_i^+ = z, \text{no bi}] \\ &\quad \cdot \Pr[\text{no bi} | \delta_i^+ = z] \cdot \Pr[\delta_i^+ = z | \delta_i^+ \geq 1], \end{aligned} \tag{4}$$

where for (4), we use the fact that $[\delta_i^+ = z, \delta_i^+ \geq 1] = [\delta_i^+ = z]$ for $z = 1, 2, \ldots, n-1$.

Given our assumption of uniformly random sector orientations, the probability of a bidirectional link existing between s_i and any of its successors s_j, denoted as $\Pr[s_j \to s_i | s_i \to s_j]$, is $\frac{\alpha}{2\pi}$; thus, the probability that no bidirectional link exists between s_i and any of its independently deployed $\delta_i^+ = z$ successors equals $(1 - \frac{\alpha}{2\pi})^z$. Therefore, given that s_i is f_1-connected:

$$\Pr[\text{no bi} | \delta_i^+ = z] = \left(1 - \frac{\alpha}{2\pi}\right)^z, \tag{5}$$

for $z = 1, 2, \cdots n-1$. Also, it is easy to see that given our unit area deployment region, we have

$$\Pr[\delta_i^- = 0 | \delta_i^+ = z, \text{no bi}] = \left(1 - \frac{\alpha r^2}{2}\right)^{n-z-1} \tag{6}$$

and

$$\begin{aligned} \Pr[\delta_i^+ = z | \delta_i^+ \geq 1] &= \frac{\Pr[\delta_i^+ = z, \delta_i^+ \geq 1]}{\Pr[\delta_i^+ \geq 1]} \\ &= \frac{\left(\frac{n\alpha r^2}{2}\right)^z e^{\frac{-n\alpha r^2}{2}}}{z!} \cdot \frac{1}{1 - e^{\frac{-n\alpha r^2}{2}}} \quad \text{for } z \geq 1, \end{aligned} \tag{7}$$

where we have made use of the fact that

$$\Pr[\delta_i^+ = z, \delta_i^+ \geq 1] = \begin{cases} \Pr[\delta_i^+ = z], & \text{for} \quad z \geq 1, \\ 0, & \text{for} \quad z = 0. \end{cases}$$

Substituting (5), (6), and (7) into (4), yields

$$\begin{aligned} p_{b|f}^i &= 1 - \sum_{z=1}^{n-1} \left(1 - \frac{\alpha r^2}{2}\right)^{n-z-1} \cdot \left(1 - \frac{\alpha}{2\pi}\right)^z \\ &\quad \cdot \left[\frac{\left(\frac{n\alpha r^2}{2}\right)^z e^{\frac{-n\alpha r^2}{2}}}{z!} \cdot \frac{1}{1 - e^{\frac{-n\alpha r^2}{2}}}\right] \end{aligned} \tag{8}$$

$$= 1 - \frac{e^{\frac{-n\alpha r^2}{2}}}{1 - e^{\frac{-n\alpha r^2}{2}}} \left(1 - \frac{\alpha r^2}{2}\right)^{n-1} \sum_{z=1}^{n-1} \frac{\left[\frac{n\alpha r^2(2\pi-\alpha)}{2\pi(2-\alpha r^2)}\right]^z}{z!}. \tag{9}$$

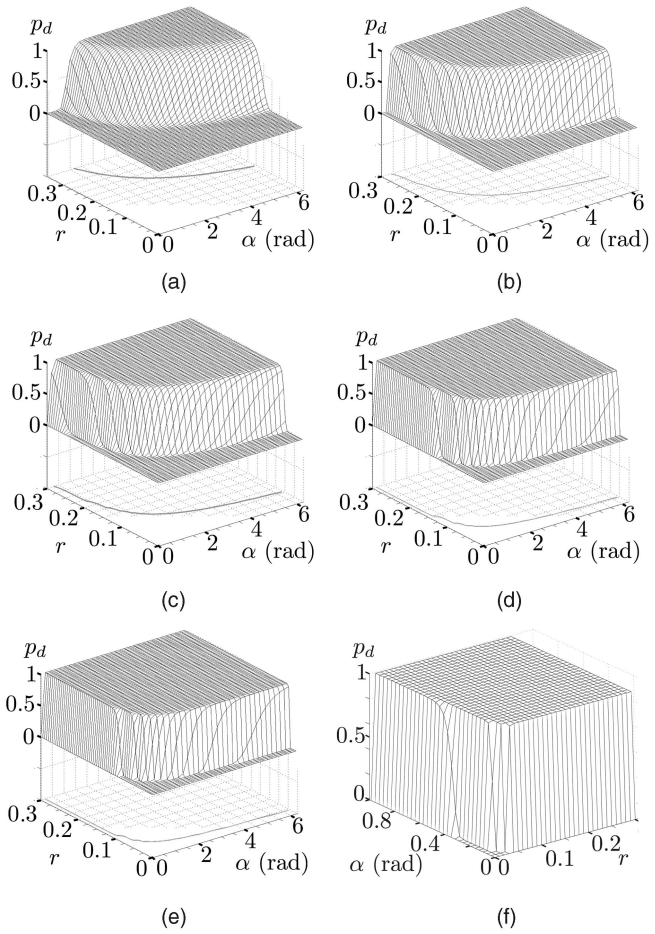

Fig. 4. Depicting the probability p_d that no isolated node occurs in $G_n(\mathcal{S}_n, \mathcal{E})$ for varying node density n. The planar line indicates (r, α) for which $p_d = 0.99$. (a) $n = 100$. (b) $n = 500$. (c) $n = 1{,}000$. (d) $n = 5{,}000$. (e) $n = 10{,}000$. (f) $n = 100{,}000$.

Employing the series approximation of an exponential for large n and $r \ll 1$, we obtain

$$p^i_{b|f} = 1 - \frac{e^{\frac{-n\alpha r^2}{2}}}{1 - e^{\frac{-n\alpha r^2}{2}}} \left(1 - \frac{\alpha r^2}{2}\right)^{n-1} \left(e^{\left\lceil \frac{n\alpha r^2(2\pi-\alpha)}{2\pi(2-\alpha r^2)} \right\rceil} - 1\right) \tag{10}$$

as the result of Lemma 4.3. □

Observe that for the omnidirectional case with $\alpha = 2\pi$, $p^i_{b|f} = 1$ as expected. That is, for the GRG model in which all links are bidirectional, if a node is f_1-connected, then, of course, it is also b_1-connected. It is clear that $p^i_{b|f} \geq p^i_b$ due to the possibility of bidirectional links.

4.4 Evaluating p^i_d and p_d

Substituting (2) and (10) into (1), and simplifying yields:

$$p^i_d = \left[1 - e^{\frac{-n\alpha r^2}{2}}\right] \left[1 - \frac{e^{\frac{-n\alpha r^2}{2}}}{1 - e^{\frac{-n\alpha r^2}{2}}} \left(1 - \frac{\alpha r^2}{2}\right)^{n-1} \cdot \left(e^{\left\lceil \frac{n\alpha r^2(2\pi-\alpha)}{2\pi(2-\alpha r^2)} \right\rceil} - 1\right)\right]. \tag{11}$$

Observe that $p^i_f \geq p^i_d$ for large n and $r \ll 1$ with equality occurring only when $\alpha = 2\pi$.

Theorem 4.4. *For $n \to \infty$ and $r \ll 1$, the probability p_d that there is no isolated node in $G_n(\mathcal{S}_n, \mathcal{E})$ is:*

TABLE 1
Minimum Communication Range r for Corresponding Parameters (n, α) that Achieves $p_d \geq 0.99$ in $G_n(\mathcal{S}_n, \mathcal{E})$

$\alpha =$	$\frac{2\pi}{9}$	$\frac{\pi}{2}$	$\frac{3\pi}{4}$	π	$\frac{3\pi}{2}$	2π
$n = 100$	0.527	0.345	0.281	0.243	0.198	0.172
$n = 500$	0.253	0.167	0.136	0.118	0.096	0.083
$n = 1000$	0.184	0.122	0.099	0.086	0.070	0.061
$n = 5000$	0.088	0.058	0.048	0.041	0.034	0.029
$n = 10000$	0.064	0.042	0.035	0.030	0.025	0.021
$n = 100000$	0.008	0.005	0.004	0.004	0.003	0.003

$$p_d = \left[1 - e^{\frac{-n\alpha r^2}{2}}\right]^n \left[1 - \frac{e^{\frac{-n\alpha r^2}{2}}}{1 - e^{\frac{-n\alpha r^2}{2}}} \left(1 - \frac{\alpha r^2}{2}\right)^{n-1} \cdot \left(e^{\left\lceil \frac{n\alpha r^2(2\pi-\alpha)}{2\pi(2-\alpha r^2)} \right\rceil} - 1\right)\right]^n. \tag{12}$$

Proof. Assuming statistical independence among the events that distinct nodes are isolated, Theorem 4.4 follows by computing p_d for n nodes as

$$p_d = \binom{n}{n} (p^i_d)^n (1 - p^i_d)^0 = (p^i_d)^n, \tag{13}$$

where the expression for p^i_d is given in (11), yielding the result of (12). □

For $\alpha = 2\pi$, we note that p_d reduces to $(1 - e^{-n\pi r^2})^n$ as obtained by Bettsetter [10]. Equation (12) is the general expression relating n, r, and α with the probability p_d that no isolated node occurs in $G_n(\mathcal{S}_n, \mathcal{E})$. Fig. 4 presents plots of p_d from (12) for a range of r and α values for different n values with the line on the $r - \alpha$ plane of each mesh plot indicating the pair values (r, α) for which with probability $p_d = 0.99$, no isolated node occurs in the WOSN. We observe that as node density n increases, network connectivity improves, and for dense networks, e.g., with $n = 100{,}000$, values as small as $(r = .01, \alpha = 6\pi/25)$ still yield a network with no isolated node.

Example 1 (simulation study). We perform a simulation-based study of a WOSN to investigate the connectivity property. Employing a uniform random generator, we position n WOSN nodes in a square planar region of area $1\ \mathrm{km}^2$, following our deployment model from Section 3. We aim to determine minimum parameter values that achieve a WOSN in which, with high probability (≥ 0.99), no node is isolated. Employing numerical analysis, from (12), we obtain the minimum r and corresponding α required for $p_d \geq 0.99$ with n given, as shown in Table 1. For example, for $n = 1{,}000$ and $\alpha = 2\pi/9, p_d \geq 0.99$ is achieved with $r \geq 0.184$ km. If, however, the WOSN nodes are only capable of achieving $r = 0.09$ km for the same α, then we need at least $\sim 5{,}000$ nodes, or at design time, we may choose to increase α to π in order to deploy the same $n = 1{,}000$ nodes and obtain the same confidence for p_d. With $n = 500$ nodes and $\alpha = 2\pi/9, \alpha = \pi/2$, and $\alpha = \pi$, we obtain $p_d \geq 0.99$ with $r \geq 0.253$ km, $r \geq 0.167$ km, and $r \geq 0.118$ km, respectively. This agrees with the

$r \geq 0.083$ km value obtained in [10] for $n = 500$ nodes in the GRG omnidirectional RF WSN scenario.

We observe that for the same confidence on p_d, doubling r allows us to reduce α by approximately a fourth. An interesting study beyond the scope of this work would involve comparing the practical cost (dollar, energy) of increasing r while reducing α (or vice versa) to determine the optimal WOSN node (r, α)-parameter configuration based on a given cost function.

4.5 K-Isolated Case

It is critical to consider K-connectivity in the design of robust secure networks that accommodate link and/or node failures and compromise due to attacks. A *K-connected network* is defined as one that remains connected after the failure of any choice of $(K-1)$ nodes. To gain insight into K-connectivity for the WOSN, we first consider the probability p_{d_K} that no directionally K-isolated node occurs, and its relationship to n, r, and α. By previous reasoning, s_i is K-connected (i.e., not K-isolated) with probability:

$$p^i_{d_K} = p^i_{f_K \cap b_K} = p^i_{f_K}.p^i_{b_K|f_K}, \tag{14}$$

where $p^i_{f_K}$ is the probability that s_i is f_K-connected and $p^i_{b_K|f_K}$ is the probability that s_i is b_K-connected, given it is f_K-connected. The probability p_{d_K} that no K-isolated node occurs in the n-node network, assuming independence among events that distinct nodes are isolated is then $p_{d_K} = (p^i_{d_K})^n$. We are left to derive $p^i_{f_K}$ and $p^i_{b_K|f_K}$.

By similar arguments, we easily extend the results of Lemmas 4.1 and 4.2 for f_1- and b_1-connectedness to the f_K- and b_K-connected cases, respectively, and conclude that the probability $p^i_{f_K} = \Pr[\delta^+_i \geq K]$ that s_i is f_K-connected is equivalent to the probability $p^i_{b_K} = \Pr[\delta^-_i \geq K]$ that s_i is b_K-connected, given as:

$$p^i_{f_K} = \Pr[\delta^+_i \geq K] = \sum_{m=K}^{n-1} \frac{e^{\frac{-n\alpha r^2}{2}} (\frac{n\alpha r^2}{2})^m}{m!} = p^i_{b_K}, \tag{15}$$

while

$$p^i_{b_K|f_K} = \Pr[\delta^-_i \geq K | \delta^+_i \geq K] = 1 - \Pr[\delta^-_i < K | \delta^+_i \geq K]. \tag{16}$$

Equations (15) and (16) yield the basis for deriving p_{d_K} by following similar arguments employed for $K = 1$. As an illustration, we derive p_{d_K} for $K = 2$.

4.5.1 Case for $K = 2$

From (15), we readily obtain that

$$\begin{aligned} p^i_{f_2} &= \Pr[\delta^+_i \geq 2] = 1 - \Pr[\delta^+_i = 0] - \Pr[\delta^+_i = 1] \\ &= 1 - e^{\frac{-n\alpha r^2}{2}} \left(1 + \frac{n\alpha r^2}{2}\right), \end{aligned} \tag{17}$$

since

$$\Pr[\delta^+_i = 0] = e^{\frac{-n\alpha r^2}{2}} \quad \text{and} \quad \Pr[\delta^+_i = 1] = \frac{n\alpha r^2}{2} e^{\frac{-n\alpha r^2}{2}}.$$

TABLE 2
Minimum Communication Range r for Corresponding Parameters (n, α) that Achieves $p_{d_2} \geq 0.99$ in $G_n(\mathcal{S}_n, \mathcal{E})$

$\alpha =$	$\frac{2\pi}{9}$	$\frac{\pi}{2}$	$\frac{3\pi}{4}$	π	$\frac{3\pi}{2}$	2π
$n = 100$	0.585	0.388	0.317	0.274	0.224	0.194
$n = 500$	0.279	0.186	0.152	0.132	0.108	0.093
$n = 1000$	0.203	0.135	0.110	0.096	0.078	0.068
$n = 5000$	0.096	0.064	0.053	0.046	0.037	0.032
$n = 10000$	0.070	0.047	0.038	0.033	0.027	0.024
$n = 100000$	0.008	0.006	0.005	0.004	0.004	0.003

From Appendix A, we obtain

$$\begin{aligned} p^i_{b_2|f_2} = 1 &- X\left(1 - \frac{\alpha r^2}{2}\right)^{n-1} \left[e^Q - Q - 1\right] \\ &- X\left(\frac{\alpha r^2}{2}\right)\left(1 - \frac{\alpha r^2}{2}\right)^{n-2} \\ &\cdot \left[(n-1)(e^Q - Q - 1) - Q(e^Q - 1)\right] \\ &- X\frac{n\alpha^2 r^2}{4\pi}\left(1 - \frac{\alpha r^2}{2}\right)^{n-2} (e^Q - 1), \end{aligned} \tag{18}$$

where

$$X = \frac{e^{\frac{-n\alpha r^2}{2}}}{1 - (1 + \frac{n\alpha r^2}{2}) e^{\frac{-n\alpha r^2}{2}}} \quad \text{and} \quad Q = \left\lceil \frac{n\alpha r^2 (2\pi - \alpha)}{2\pi(2 - \alpha r^2)} \right\rceil.$$

Observe again that $p^i_{b_2|f_2} = 1$ when $\alpha = 2\pi$, as expected, since in a bidirectional network, given $\delta^+_i \geq 2$, then with probability 1, $\delta^-_i \geq 2$. It is now trivial to obtain the probability $p^i_{d_2}$ that s_i is not 2-isolated as $p^i_{d_2} = p^i_{f_2}.p^i_{b_2|f_2}$; and the probability that no 2-isolated node occurs in the network assuming independence is then obtained as $p_{d_2} = (p^i_{d_2})^n$ by simple substitution. We have omitted the actual analytical expressions for $p^i_{d_2}$ and p_{d_2} as they appear repetitive. For $\alpha = 2\pi$ representing the omnidirectional case, $p_{d_2} = [1 - e^{\frac{-n\alpha r^2}{2}}(1 + \frac{n\alpha r^2}{2})]^n$.

Example 2 (simulation study). We consider a simulation setup similar to Example 1 with the aim of achieving a WOSN in which almost surely no 2-isolated node occurs; we say that event A occurs almost surely if the probability of event A, Pr[A] ≥ 0.99. Table 2 presents the minimum r corresponding to preselected α and n for which $p_{d_2} \geq 0.99$. We observe that for $n = 5{,}000$ and $\alpha = \pi/2, p_{d_2} \geq 0.99$ for $r \geq 0.064$ km. However, if the nodes are capable of r up to 0.14 km, then for the same α and p_{d_2}, we require only 1,000 nodes. On the other hand, if our nodes are only capable of $\alpha = 2\pi/9$ and $r = 0.07$ km, then we need at least 10,000 nodes to achieve the same p_{d_2}. Our expression yields $r \geq 0.093$ km for the omnidirectional network scenario, with $n = 500$ as observed in [10]. Compared to the $K = 1$ case, larger values for the corresponding minimum r and α are required to achieve the same p_{d_2}.

4.6 Simulations and Discussions

In this section, we perform a simulation-based study to empirically determine p_d (Sim) and compare it with

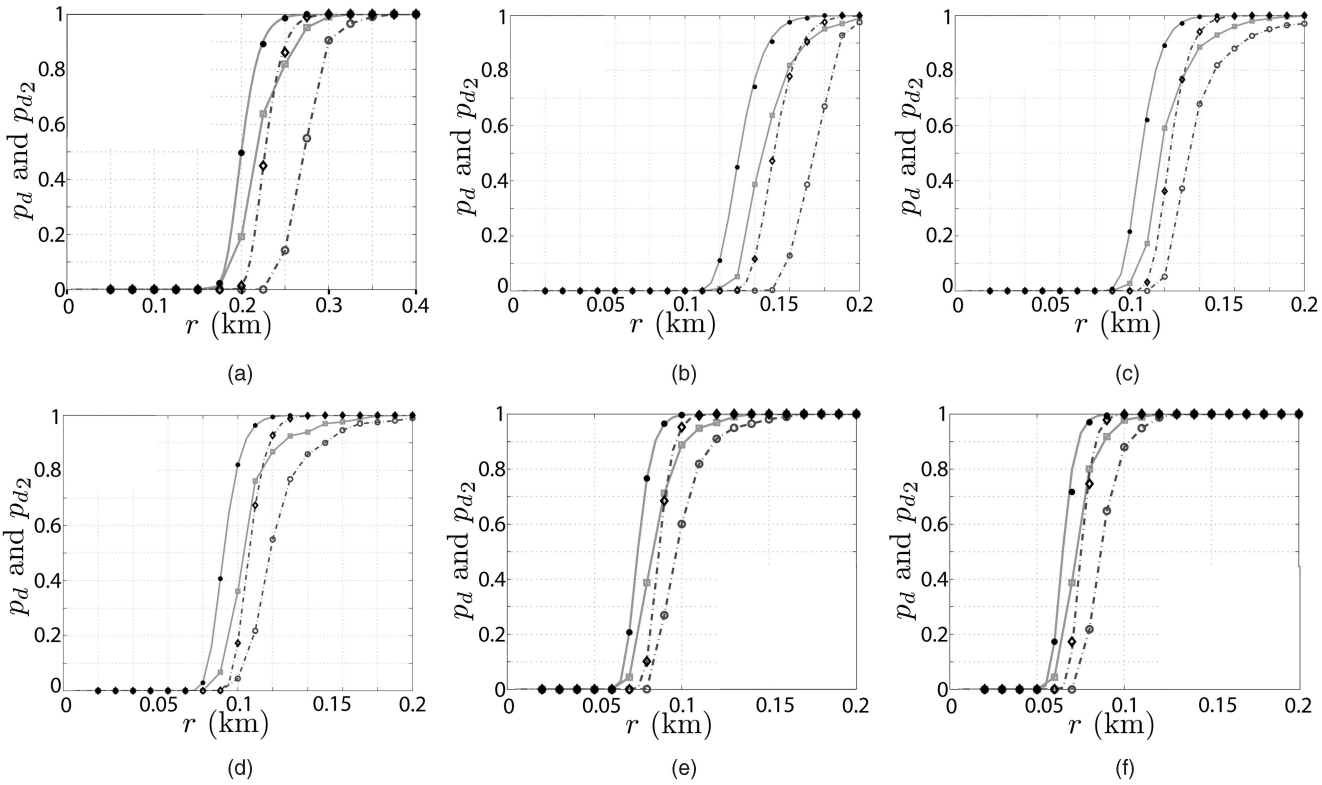

Fig. 5. Analytical p_d (Anal), simulation p_d for euclidean (Eucl), and Toroidal (Toro) metrics for $K = 1, 2, n = 500$, with varying r and α; p_d-Anal, p_d-Eucl, and p_d-Toro represented by solid, solid-square, and closed-circle annotations, respectively; p_{d_2}-Anal, p_{d_2}-Eucl, and p_{d_2}-Toro represented by dash-dot, dash-dot-circle, and diamond annotations, respectively. (a) $\alpha = \frac{2\pi}{9}$. (b) $\alpha = \frac{\pi}{2}$. (c) $\alpha = \frac{3\pi}{4}$. (d) $\alpha = \pi$. (e) $\alpha = \frac{3\pi}{2}$. (f) $\alpha = 2\pi$.

analytical curves for p_d (Anal) obtained for $K = 1, 2$. We employ MATLAB software to simulate a WOSN in which the set $\mathcal{S}_n$ of n WOSN nodes is randomly positioned and oriented according to a uniform distribution in a planar square region of unit area $1\ \text{km}^2$. For $n = 500$ nodes, we employ six representative α values ($\frac{2\pi}{9}, \frac{\pi}{2}, \frac{3\pi}{4}, \pi, \frac{3\pi}{2}, 2\pi$), and r ranging from 0 to 0.2 km (except for $\alpha = \frac{2\pi}{9}$, where we have used a wider range of r values from 0 to 0.4 km in order to observe salient changes in p_d). We then obtain the adjacency matrix $\mathcal{E}$ of the resulting WOSN employing the conventional euclidean distance metric to determine the successors and predecessors of each node, and study the node isolation property of $G_n(\mathcal{S}_n, \mathcal{E})$ by observing the neighborhood relationships reflected in $\mathcal{E}$. Note that it is sufficient to compute successors of each node in populating $\mathcal{E}$, as predecessor relationships are derived by reversing successor links. Analysis to determine the successors of a node is presented in the Appendix. For each set of network parameters, our simulations are repeated 1,000 times to yield an acceptable statistical confidence of the obtained results, and p_d measured for each random network topology. We obtain an empirical average of p_d by counting the number of *directionally isolated nodes* n_I in each simulation scenario and computing p_d as $(1 - \frac{n_I}{n})$, averaged over the 1,000 random trials.

We conduct a second set of simulations in which $\mathcal{E}$ is computed using the Toroidal distance metric to obtain p_d without border effects. With the Toroidal metric, nodes at a border of the deployment region are modeled as being adjacent to nodes at the opposite border, creating a wrap around effect so that the flat simulation area becomes a torus. In our plots, we refer to p_d-Eucl and p_d-Toro as simulation plots obtained for p_d employing the euclidean and Toroidal distance metrics, respectively. We also conduct a third set of simulations to investigate the directional 2-isolation property of WOSNs, and derive empirical curves for p_{d_2}-Eucl and p_{d_2}-Toro to compare with analytically derived p_{d_2}.

Fig. 5 depicts plots of p_d and p_{d_2}, illustrating the simulation results qualitatively follow the analytical plots, with p_d-Toro almost exactly matching p_d-Anal as expected. We observe that p_d-Eucl does not exactly coincide with p_d-Anal due to adverse border effects and a finite simulation region; and for smaller α values, the disparity between p_d-Anal and p_d-Eucl grows, due to the border effects becoming more severe, as nodes at the boundary become isolated with a higher probability than for larger α values. Compensating for this boundary effect with p_d-Toro, the desired result of an excellent matchup with p_d-Anal occurs. Also, we note that as n grows to form a denser network, the analytical and simulation plots agree more closely, due to the approximations made for $n \to \infty$ in the analytic derivations. Observe that the p_{d_2} curves perform similarly so that as $\alpha \to 2\pi$, the simulation p_ds more closely approach analytical p_ds, more so for $K = 2$ than $K = 1$. In both cases, however, eliminating border effects results in a high degree of matchup to analytical predictions.

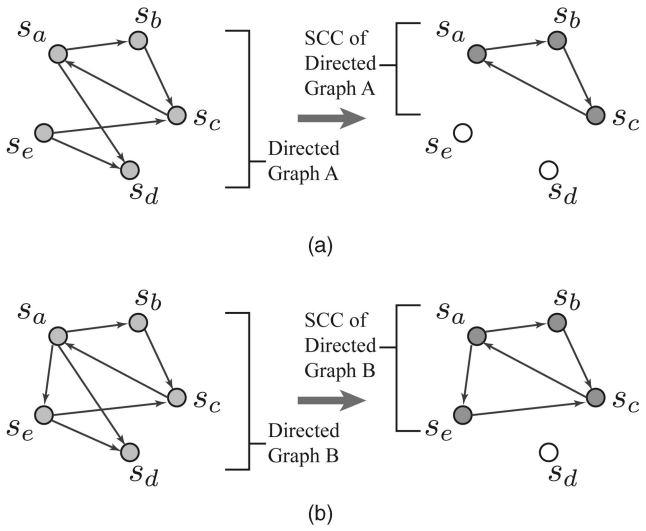

Fig. 6. SCCs. (a) For graph A, $p_c = 3/5$. (b) For graph B, $p_c = 4/5$.

5 Empirical Studies

5.1 WOSN Connectivity and Node Isolation

In this section, we investigate the relationship between the connectivity property of the WOSN and the node isolation property. As previously noted in Section 4, recent work [10] has shown that for large n, the probability p_c that the RF WSN is connected is tightly upper bounded by p_d for $n \to \infty$ and probabilities close to one. We empirically verify this property that also holds for WOSNs modeled as RSSGs, while studying the effect varying r and α values have on p_c.

To determine p_c by simulations, we obtain the number of nodes n_c in the WOSN's largest *strongly connected component* (SCC) $G_n^c(\mathcal{S}_n, \mathcal{E}) \subset G_n(\mathcal{S}_n, \mathcal{E})$ as a fraction of n. The directed subgraph $G_n^c(\mathcal{S}_n, \mathcal{E})$ forms the largest connected partition of the WOSN such that any pair of nodes in $G_n^c(\mathcal{S}_n, \mathcal{E})$ are pairwise connected. Fig. 6 depicts examples of the SCC of two 5-node directed graphs A and B, with p_c equivalent to $\frac{3}{5}$ and $\frac{4}{5}$, respectively. We employ the well-known Kosaraju's algorithm [29] which efficiently implements a depth-first-search (DFS) algorithm [30] to determine $G_n^c(\mathcal{S}_n, \mathcal{E})$ in our simulations. Kosaraju's algorithm uses the fact that the transpose graph of a directed graph has exactly the same SCC as the original graph.

Similar to the MATLAB simulation scenario used to study node isolation in Section 4.6, we first generate an n-node random topology of the WOSN over a square region of unit area $1\ \mathrm{km}^2$. For $n = 500$, six representative α values, and r varying, we repeat our simulations 1,000 times to yield an acceptable confidence of obtain results. We measure empirical values for p_c as the ratio n_c/n for each trial, averaged over the 1,000 random topologies, where $G_n^c(\mathcal{S}_n, \mathcal{E})$ is obtained using Kosaraju's algorithm. Because Kosaraju's algorithm is $O(|\mathcal{E}| n \log n)$, extensive simulation time is required to determine p_c, even with the use of supercomputing facilities especially for large r and α values for which $\mathcal{E}$ is dense.

In Fig. 7, comparing plots of empirically derived p_c (using both an euclidean and a Toroidal distance metric), with p_d-Anal and p_d-Sim, for preselected α values, we observe that for probability values close to 1, the property that $p_c \approx p_d$ holds, when the Toroidal distance metric is used to compensate for boundary effects. This implies that for probabilities larger than about 0.96, parameter values obtained for the curve of p_d serve as a good approximation for attaining the same p_c confidence. In a real-world application, this approximation would hold true with dense networks and large deployment regions that minimize boundary effects. It is noteworthy that our results are consistent with the conclusions of [10]. That is, for WOSNs, p_d is a tight upper bound for p_c for $n \to \infty$ and probabilities close to 1, with the bound getting tighter as α increases. That is, as $\alpha \to 2\pi$, p_c does a much better job at approaching p_d, especially for probability values close to 1.

An interesting phenomenon observed for p_d and p_c is their decreasing "phase transition" or percolation region as $\alpha \to 2\pi$. In the phase transition phenomenon, typically observed for random graphs [9], p_c transitions rapidly from 0 (i.e., network is disconnected with probability 1) to 1 (i.e., network is connected with probability 1). For example, for $\alpha = \frac{2\pi}{9}, \pi$ and 2π, while $p_c = 0$ for $r = 0.20$, 0.08, and 0.06 km, respectively, $p_c = 1$ for $r = 0.35$, 0.18, and 0.12 km, respectively. That is, for $\alpha = \frac{2\pi}{9}, \pi$ and 2π, the "phase transition" spans a distance of 0.15, 0.10, and 0.06 km, respectively. In conclusion, we state the following:

Lemma 5.1. *For n WOSN nodes randomly distributed and oriented on the planar unit area square according to a uniform distribution, let r_c and r_d denote the minimum r at which the network graph $G_n(\mathcal{S}_n, \mathcal{E})$ is connected and attains no isolated node, respectively. Then, with high probability,* $\Pr[r_c = r_d] \to 1 \quad \text{as} \quad n \to \infty \quad \text{and} \quad \alpha \to 2\pi.$

We conclude this section by summarizing insights on the node isolation and connectivity properties for WOSNs gained from our analysis and simulations, compared to the $\alpha = 2\pi$ case.

1. A linear change in r produces a more significant impact on p_d than a linear change in α.
2. Similar to the $\alpha = 2\pi$ case, there is a critical value of r above which the network will almost surely have no isolated nodes. This natural trend is preserved for RSSG networks as it is for GRG networks. We also observe that the "phase transition" regions of p_c and p_d versus r increases as α gets smaller.
3. For K-connectivity of the WOSN, as K grows, it can be projected that significantly larger values of r will be required to maintain connectivity for lower values of α. For WOSNs in which a fraction of nodes may fail or be corrupted, such performance motivates the need for a hybrid or clustered heterogeneous paradigm.
4. The results of this paper have demonstrated practical design solutions for node isolation and network disconnectedness, which has been one of the major hurdles for the deployment of WOSNs. The potential for guaranteeing connectivity in WOSNs provides further support for random deployment of emerging hybrid RF/FSO or directional RF systems [12].

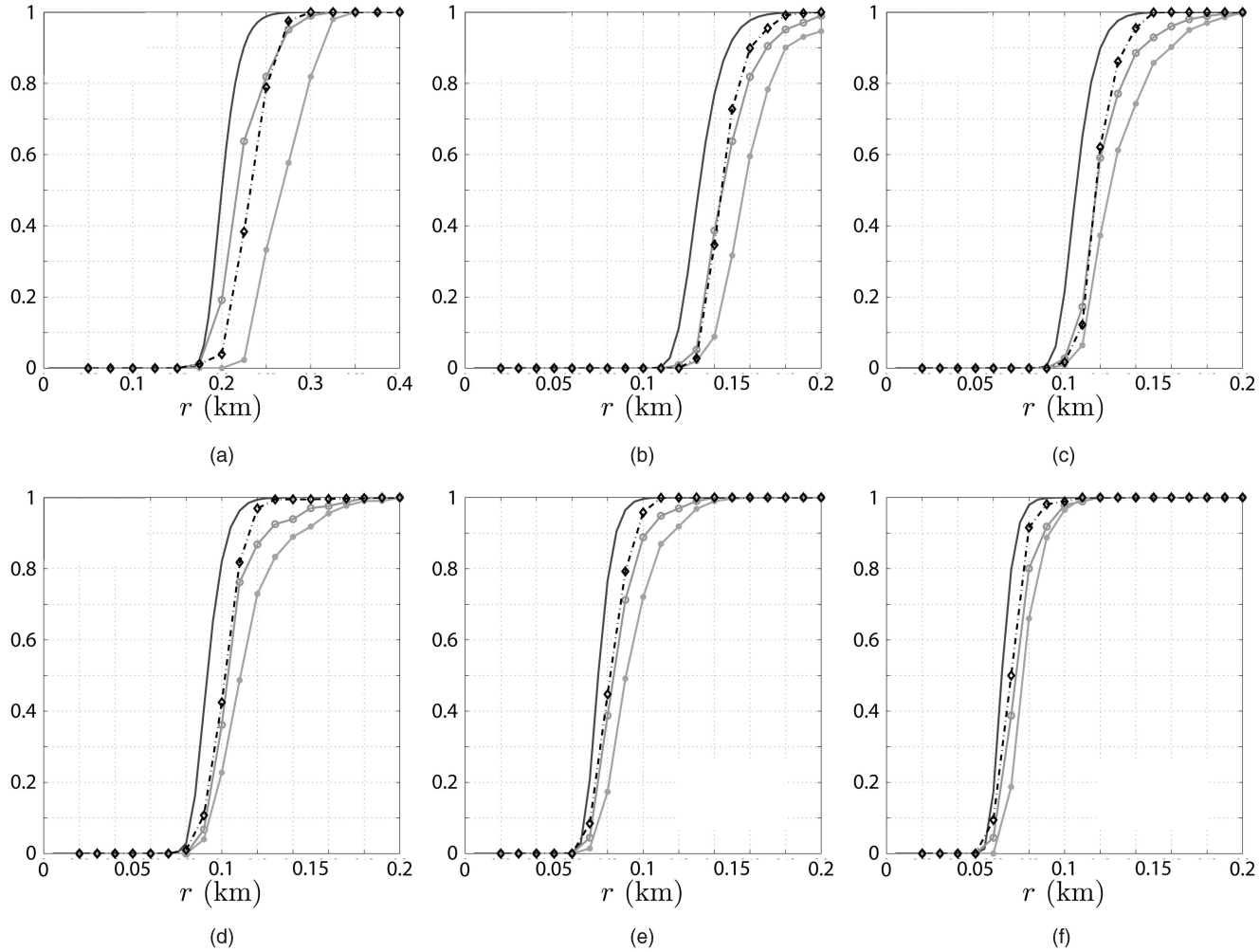

Fig. 7. Probability p_c that the network is connected and the probability p_d that there is no isolated network node for both analytic and simulated cases; p_d-Anal, p_d-Eucl, p_c-Eucl, and p_c-Toro are represented by the solid, solid-open circle, solid-closed circle, and dash-dot-diamond annotations, respectively. (a) $\alpha = \frac{2\pi}{9}$. (b) $\alpha = \frac{\pi}{2}$. (c) $\alpha = \frac{3\pi}{4}$. (d) $\alpha = \pi$. (e) $\alpha = \frac{3\pi}{2}$. (f) $\alpha = 2\pi$.

5.2 Impact of Hierarchy and Clustering

An evaluation of the impact of clustering on the connectivity of WOSNs is motivated by the naturally hierarchical communication model of WOSNs, consisting mainly of either base station-to-nodes or nodes-to-base station traffic [27]. In a cluster-based WOSN as previously described, a fraction of the nodes act as CHs that send and receive data directly to and from the base station, respectively, on behalf of the other (non-CHs) nodes [26]. The CHs may have different hardware requirements than the non-CH nodes, but it is possible that any node can become a CH with a bidirectional link to the base station by using hardware such as CCRs [26].

Hierarchically, the base station forms the highest layer, the CHs constitute the middle layer, while the non-CHs form the lowest layer of the WOSN. Clustered RF WSNs have been studied with regard to improving energy, power and topology control, scalability, load balancing, data aggregation, and fault-tolerance and routing efficiency [31], [32], [27], [33], [34].

Recall that by employing the base station as a "middle man," we assume that a virtual backbone grid connects all CHs via the base station so that $\mathcal{E}(k,l) = \mathcal{E}(l,k) = 1, \forall s_k^*, s_l^* \in \mathcal{CH}$. We define the WOSN *hierarchical connectivity* (H-connectivity) property as the connectivity of the *supergraph* $G_n^s(\mathcal{S}_n, \mathcal{E}^s) \supseteq G_n(\mathcal{S}_n, \mathcal{E})$ formed by adding edges [18] between all pairs of nodes in $\mathcal{CH}$. In this model, the CHs are equivalent to *articulation nodes* which form a *cut set* for the SCC of $G_n^s(\mathcal{S}_n, \mathcal{E}^s)$ with high probability. This implies that removal of the set $\mathcal{CH}$ will most likely result in disconnection of $G_n^s(\mathcal{S}_n, \mathcal{E}^s)$. An implication of an H-connected WOSN is that all nodes can send and receive data with the base station, conforming to the desired traffic pattern of WSNs.

Within this context, the question we answer is, what is the impact of the fraction of CH nodes p_{CH} on the H-connectivity property of $G_n(\mathcal{S}_n, \mathcal{E})$? More specifically, how can we choose p_{CH} such that with a given probability p_H, the network is H-connected. The answer to this question is crucial in determining the fraction of "special" nodes that must be manufactured and deployed as CHs during design phase, to achieve a desired p_H, where p_{CH} is then an additional tunable network parameter to achieve a more flexible network design.

We empirically evaluate the effect of clustering on H-connectivity. Similar to previous simulations, 1,000 random topologies of a 500-node network are generated and evaluated to yield acceptable confidence on obtained empirical results. In this scenario, nodes are designated as CHs with probability p_{CH} set to three representative

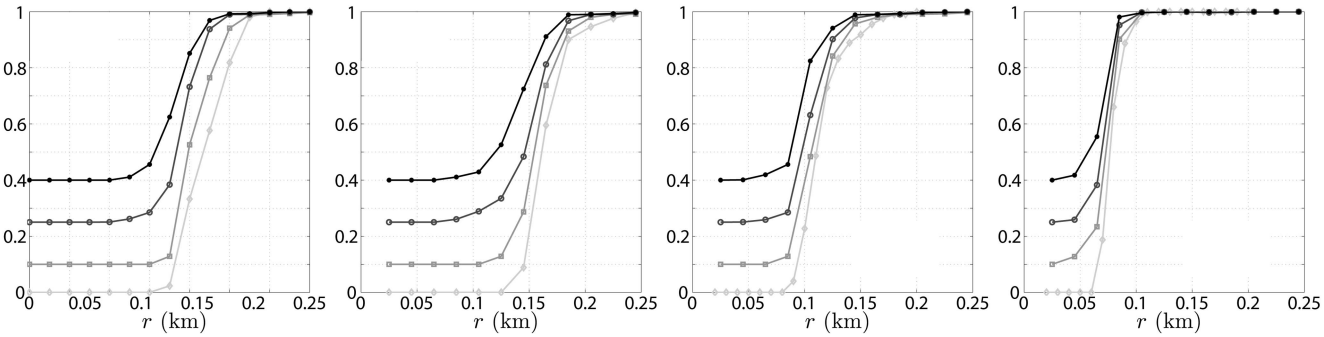

Fig. 8. Plots of p_{hc} compared to p_c for varying p_{CH}; p_c (no clustering), p_H ($p_{CH} = 0.1$), p_H ($p_{CH} = 0.25$), and p_H ($p_{CH} = 0.4$) are represented by the diamond, square, open circle, and dotted annotations, respectively. (a) $\alpha = \frac{2\pi}{9}$. (b) $\alpha = \frac{\pi}{2}$. (c) $\alpha = \pi$. (d) $\alpha = 2\pi$.

values of 10, 25, and 40 percent, and the adjacency matrix of $G_n^s(\mathcal{S}_n, \mathcal{E}^s)$ is obtained by updating $\mathcal{E}$ to reflect the additional links between all CHs. We compute p_H as the ratio of the number of nodes in the SCC of $G_n^s(\mathcal{S}_n, \mathcal{E}^s)$ to n, and obtain empirical values for p_H as the average across the 1,000 trials.

Fig. 8 depicts plots of p_H compared to p_c for the different P_{CH} values. We observe that for all α values, clustering remarkably improves network connectivity. For example, for $\alpha = \frac{2\pi}{9}$, we observe that $p_c = 0.33$ for $r = 0.25$, while $p_H = 0.52$, 0.72, and 0.85, respectively, with corresponding p_{CH} values of 10, 25, and 40 percent. Consider, for example, a WOSN deployed within a unit area (1 km^2) planar region. The network owner can only afford to deploy a limited number of nodes, say 500 nodes, each node possessing a communication radius r and angle α of 0.15 m and $\frac{\pi}{2}$, respectively. Under this scenario, he is only guaranteed network connectivity of about 20 percent. If, however, 25 percent of nodes are equipped to function as CHs, the connectivity of the network improves to 60 percent. Further, with 40 percent of nodes designated as CHs, the network connectedness attains almost 80 percent (see Fig. 8b). Future work for practical cost may consider the trade-off between enhancing a node's capability to function as a CH versus deploying more of the lower level nodes be considered. We will also address the problem of determining analytic bounds relating the likelihood of connectivity to p_{CH} and intend to consider the problems of connectivity in hierarchal mobile WOSNs employing the concept of *dynamic* GRGs [35].

6 Concluding Remarks

In this paper, we employed a probabilistic approach to investigate the node isolation property for WOSNs and its relation to the connectivity of the network. We derived an analytical expression giving the relationship among the physical layer network parameters r, n, and α of a WOSN such that with high probability p_d, an isolated node does not occur in the network. Our results are particularly significant in view of recent work [10] which has shown that the probability that there is no isolated node provides a tight lower bound to the probability that the network is connected. We showed that a similar conclusion is applicable to the WOSN modeled as an RSSG, and is especially valid as $\alpha \to 2\pi$. The results of this paper are vital as a starting platform toward determining practical parameter design values in order to achieve a highly connected network.

Appendix A
Evaulating $p^i_{b_2|f_2}$

We employ the following argument to derive $p^i_{b_2|f_2}$, where we denote the event that s_i has exactly one bidirectional link as [1 bi], and the event that s_i has at least two bidirectional links as [a.l. 2 bi]:

$$\begin{aligned} p^i_{b_2|f_2} &= \Pr[\delta_i^- \geq 2 | \delta_i^+ \geq 2] = 1 - \Pr[\delta_i^- < 2 | \delta_i^+ \geq 2] \\ &= 1 - \big\{\Pr[\delta_i^- = 0 | \delta_i^+ \geq 2] + \Pr[\delta_i^- = 1 | \delta_i^+ \geq 2]\big\} \\ &= 1 - \big\{\Pr[\delta_i^- = 0 | \delta_i^+ \geq 2, \text{no bi}] \cdot \Pr[\text{no bi}] \\ &\quad + \Pr[\delta_i^- = 1 | \delta_i^+ \geq 2, \text{no bi}] \cdot \Pr[\text{no bi}]\big\} \\ &\quad - \big\{\Pr[\delta_i^- = 0 | \delta_i^+ \geq 2, \text{a.l. 1 bi}] \cdot \Pr[\text{a.l. 1 bi}] \\ &\quad + \Pr[\delta_i^- = 1 | \delta_i^+ \geq 2, 1 \text{ bi}] \cdot \Pr[1 \text{ bi}]\big\} \\ &\quad - \Pr[\delta_i^- = 1 | \delta_i^+ \geq 2, \text{a.l. 2 bi}] \cdot \Pr[\text{a.l. 2 bi}]. \end{aligned}$$

But again, due to contradicting events, $\Pr[\delta_i^- = 0 | \delta_i^+ \geq 2, \text{a.l. 1 bi}] = \Pr[\delta_i^- = 1 | \delta_i^+ \geq 2, \text{a.l. 2 bi}] = 0$, so that:

$$\begin{aligned} p^i_{b_2|f_2} &= 1 - \Pr[\delta_i^- = 0 | \delta_i^+ \geq 2, \text{no bi}] \cdot \Pr[\text{no bi}] \\ &\quad - \Pr[\delta_i^- = 1 | \delta_i^+ \geq 2, \text{no bi}] \cdot \Pr[\text{no bi}] \\ &\quad - \Pr[\delta_i^- = 1 | \delta_i^+ \geq 2, 1 \text{ bi}] \cdot \Pr[1 \text{ bi}]. \end{aligned} \tag{19}$$

To obtain the accurate analytical representations, we expand the three parts of (19) for $z = 2, 3, \cdots n-1$ as follows:

$$\begin{aligned} p^i_{b_2|f_2} &= 1 - \sum_{z=2}^{n-1} \big\{\Pr[\delta_i^- = 0 | \delta_i^+ = z, \text{no bi}] \\ &\quad \cdot \Pr[\text{no bi} | \delta_i^+ = z] \cdot \Pr[\delta_i^+ = z | \delta_i^+ \geq 2]\big\} \\ &\quad - \sum_{z=2}^{n-1} \big\{\Pr[\delta_i^- = 1 | \delta_i^+ = z, \text{no bi}] \\ &\quad \cdot \Pr[\text{no bi} | \delta_i^+ = z] \cdot \Pr[\delta_i^+ = z | \delta_i^+ \geq 2]\big\} \\ &\quad - \sum_{z=2}^{n-1} \big\{\Pr[\delta_i^- = 1 | \delta_i^+ = z, 1 \text{ bi}] \\ &\quad \cdot \Pr[1 \text{ bi} | \delta_i^+ = z] \cdot \Pr[\delta_i^+ = z | \delta_i^+ \geq 2]\big\}. \end{aligned} \tag{20}$$

There are four terms in (20). The first term is 1, the second, third, and fourth summation terms are denoted as $T2$, $T3$, and $T4$, respectively.

We know the closed-form expressions for the following probabilities, for $z = 2, 3, \ldots n-1$:

$$\Pr[\text{no bi}|\delta_i^+ = z] = \left(1 - \frac{\alpha}{2\pi}\right)^z, \tag{21}$$

$$\Pr[1 \text{ bi}|\delta_i^+ = z] = z\frac{\alpha}{2\pi}\left(1 - \frac{\alpha}{2\pi}\right)^{z-1}, \tag{22}$$

$$\Pr[\delta_i^- = 0|\delta_i^+ = z, \text{no bi}] = \left(1 - \frac{\alpha r^2}{2}\right)^{n-z-1}, \tag{23}$$

$$\begin{aligned}\Pr[\delta_i^- = 1|\delta_i^+ = z, \text{no bi}] &= (n-z-1)\left(\frac{\alpha r^2}{2}\right) \\ &\cdot \left(1 - \frac{\alpha r^2}{2}\right)^{n-z-2},\end{aligned} \tag{24}$$

$$\Pr[\delta_i^- = 1|\delta_i^+ = z, 1 \text{ bi}] = \left(1 - \frac{\alpha r^2}{2}\right)^{n-z-1}, \tag{25}$$

and

$$\begin{aligned}\Pr[\delta_i^+ = z|\delta_i^+ \geq 2] &= \frac{\Pr[\delta_i^+ = z, \delta_i^+ \geq 2]}{\Pr[\delta_i^+ \geq 2]} \\ &= \frac{\left(\frac{n\alpha r^2}{2}\right)^z e^{\frac{-n\alpha r^2}{2}}}{z!\left[1 - e^{\frac{-n\alpha r^2}{2}}\left(1 + \frac{n\alpha r^2}{2}\right)\right]},\end{aligned} \tag{26}$$

where

$$\Pr[\delta_i^+ = z, \delta_i^+ \geq 2] = \begin{cases} \Pr[\delta_i^+ = z], & \text{for} \quad z \geq 2, \\ 0, & \text{for} \quad z = 0, 1, \end{cases}$$

and

$$\Pr[\delta_i^- = k] = \binom{n-z-1}{k}\left(\frac{\alpha r^2}{2}\right)^k\left(1 - \frac{\alpha r^2}{2}\right)^{n-z-1-k}.$$

Substituting (21), (23), and (26) into the second term of (20), we obtain

$$\begin{aligned}T2 &= X\sum_{z=2}^{n-1}\frac{\left(1 - \frac{\alpha}{2\pi}\right)^z\left(1 - \frac{\alpha r^2}{2}\right)^{n-1-z}\left(\frac{n\alpha r^2}{2}\right)^z}{z!} \\ &= X\left(1 - \frac{\alpha r^2}{2}\right)^{n-1}\sum_{z=2}^{n-1}\frac{\left(\frac{n\alpha r^2(2\pi-\alpha)}{2\pi(2-\alpha r^2)}\right)^z}{z!} \\ &= X\left(1 - \frac{\alpha r^2}{2}\right)^{n-1}\sum_{z=2}^{n-1}\frac{Q^z}{z!} \\ &= X\left(1 - \frac{\alpha r^2}{2}\right)^{n-1}\left(e^Q - Q - 1\right),\end{aligned} \tag{27}$$

where

$$X = \frac{e^{\frac{-n\alpha r^2}{2}}}{1 - (1 + \frac{n\alpha r^2}{2})e^{\frac{-n\alpha r^2}{2}}} \quad \text{and} \quad Q = \left[\frac{n\alpha r^2(2\pi - \alpha)}{2\pi(2 - \alpha r^2)}\right],$$

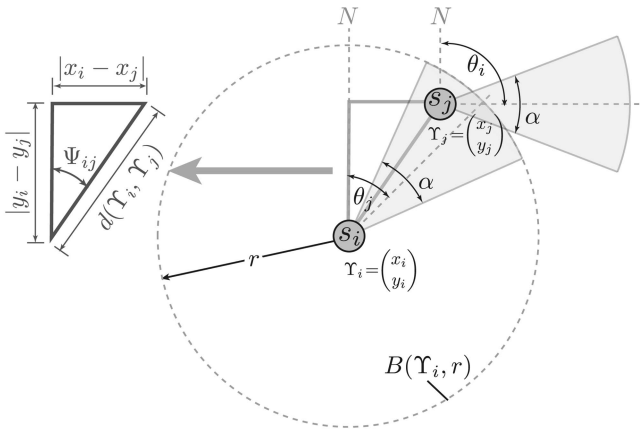

Fig. 9. Geometry for computing successors ($s_i \rightarrow s_j$) based on nodes' relative position and orientation.

and the series approximation of the exponential is employed assuming large n and $r \ll 1$. Similarly, substituting (21), (24), and (26) into the third term of (20) and simplifying, we obtain

$$\begin{aligned}T3 &= X\frac{\alpha r^2}{2}\left(1 - \frac{\alpha r^2}{2}\right)^{n-2} \\ &\cdot \left\{(n-1)(e^Q - Q - 1) - Q(e^Q - 1)\right\}.\end{aligned} \tag{28}$$

Again, we substitute (22), (24), and (26) into the fourth term of (20) and simplify to obtain for large n and $r \ll 1$ that:

$$\begin{aligned}T4 &= X\frac{\alpha}{2\pi}\sum_{z=2}^{n-1}\frac{z\left(1 - \frac{\alpha}{2\pi}\right)^{z-1}\left(1 - \frac{\alpha r^2}{2}\right)^{n-z-1}\left(\frac{n\alpha r^2}{2}\right)^z}{z!} \\ &= X\frac{n\alpha^2 r^2}{4\pi}\left(1 - \frac{\alpha r^2}{2}\right)^{n-2}\left(e^Q - 1\right).\end{aligned} \tag{29}$$

Substituting expressions for $T2, T3$, and $T4$ into (19), we finally obtain

$$\begin{aligned}p_{b_2|f_2}^i &= 1 - X\left(1 - \frac{\alpha r^2}{2}\right)^{n-1}\left[e^Q - Q - 1\right] \\ &- X\left(\frac{\alpha r^2}{2}\right)\left(1 - \frac{\alpha r^2}{2}\right)^{n-2} \\ &\cdot \left[(n-1)\left(e^Q - Q - 1\right) - Q(e^Q - 1)\right] \\ &- X\frac{n\alpha^2 r^2}{4\pi}\left(1 - \frac{\alpha r^2}{2}\right)^{n-2}\left(e^Q - 1\right).\end{aligned} \tag{30}$$

APPENDIX B
DETERMINING SUCCESSOR RELATIONSHIPS

Consider a reference origin (0,0) and reference orientation, denoted as N in Fig. 9. The euclidean distance between two nodes s_i and s_j is

$$d(s_i, s_j) = \sqrt{(x_i - x_j)^2 + (y_i - y_j)^2},$$

and the angle between s_i and s_j is

$$\Psi_{ij}^T = \min\left[|\Theta_i - \Psi_{ij}|, |\Theta_i + 2\pi - \Psi_{ij}|, |\Theta_i - 2\pi - \Psi_{ij}|\right],$$

where

$$\Psi_{ij} = \arccos \frac{d(y_j, y_i)}{d(\Upsilon_j, \Upsilon_i)}.$$

Then, $s_i \rightarrow s_j$ illustrated in Fig. 9 if $d(s_i, s_j) \leq r$ and $|\Theta_i - \Psi_{ij}^T| \leq \frac{\alpha}{2}$.

APPENDIX C
COMPUTING TOROIDAL DISTANCES

The Toroidal distance metric is employed to eliminate border effects [10]. If $d(\binom{x_i}{y_i}, \binom{x_j}{y_j})$ denotes the usual euclidean distance between two point $\binom{x_i}{y_i}$ and $\binom{x_j}{y_j}$ on a bounded area $[0, x_{max}][0, y_{max}]$. Then, the Toroidal distance $d_T(s_1, s_2)$ between nodes s_1 and s_2 equals:

$$\begin{aligned}
\min\Bigg[& d\left(\binom{x_i}{y_i}, \binom{x_j}{y_j}\right), d\left(\binom{x_i + x_{max}}{y_i}, \binom{x_j}{y_j}\right), \\
& d\left(\binom{x_i - x_{max}}{y_i}, \binom{x_j}{y_j}\right), \\
& d\left(\binom{x_i}{y_i + y_{max}}, \binom{x_j}{y_j}\right), d\left(\binom{x_i}{y_i - y_{max}}, \binom{x_j}{y_j}\right), \\
& d\left(\binom{x_i + x_{max}}{y_i + y_{max}}, \binom{x_j}{y_j}\right), \\
& d\left(\binom{x_i + x_{max}}{y_i - y_{max}}, \binom{x_j}{y_j}\right), d\left(\binom{x_i - x_{max}}{y_i + y_{max}}, \binom{x_j}{y_j}\right), \\
& d\left(\binom{x_i - x_{max}}{y_i - y_{max}}, \binom{x_j}{y_j}\right)\Bigg].
\end{aligned}$$

Note that $d_T(s_i, s_j) \leq d(s_i, s_j)$, and $s_i \rightarrow s_j$ if $d_T(s_i, s_j) \leq r$ and $|\Theta_i - \Psi_{ij}^T| \leq \frac{\alpha}{2}$.

ACKNOWLEDGMENTS

The authors would like to thank the three anonymous reviewers and the Associate Editor, Professor Prasant Mohapatra, for their valuable feedback. They acknowledge several hours of use on The Texas A&M Supercomputing Facility (http://sc.tamu.edu/). They also thank members of the SeMANTIC research group at Texas A&M University for lively discussions and insightful ideas. They especially appreciate the careful proof reading of their manuscript and verification of their analytical derivations by Julien Jainsky. This research was partially supported by the US National Science Foundation under grants ECCS-0735114 and EEC-0649142.

REFERENCES

[1] I.F. Akyildiz, W. Su, Y. Sankarasubramaniam, and E. Cayirci, "A Survey on Sensor Networks," *IEEE Comm. Magazine,* vol. 40, no. 8, pp. 102-114, Aug. 2002.

[2] P. Gupta and P.R. Kumar, "Critical Power for Asymptotic Connectivity in Wireless Networks," *Stochastic Analysis, Control, Optimization and Applications,* pp. 547-566, Birkhäuser, 1998.

[3] R. Ramanathan, "On the Performance of Ad Hoc Networks with Beamforming Antennas," *Proc. ACM MobiHoc,* June 2001.

[4] A. Saha and D. Johnson, "Routing Improvement Using Directional Antennas in Mobile Ad Hoc Networks," *Proc. IEEE Global Telecomm. Conf. (GLOBECOM '04),* 2004.

[5] K. Sudaresan and R. Sivakumar, "On the Medium Access Control Problem in Ad-Hoc Networks with Smart Antennas," *Proc. ACM MobiHoc,* June 2003.

[6] Y. Wu, L. Zhang, Y. Wu, and Z. Niu, "Interest Dissemination with Directional Antennas for Wireless Sensor Networks with Mobile Sinks," *Proc. Fourth Int'l Conf. Embedded Networked Sensor Systems (Sensys '06),* 2006.

[7] J. Díaz, J. Petit, and M. Serna, "A Random Graph Model for Optical Networks of Sensors," *IEEE Trans. Mobile Computing,* vol. 2, no. 3, pp. 186-196, July-Sept. 2003.

[8] *Random Geometric Graphs,* M.D. Penrose, ed. Oxford Univ. Press, 2003.

[9] P. Erdos and A. Renyi, "On the Evolution of Random Graphs," *Math. Inst. of Hungary Academy of Science,* vol. 5, pp. 17-61, 1960.

[10] C. Bettstetter, "On the Minimum Node Degree and Connectivity of a Wireless Multihop Network," *Proc. Third ACM Int'l Symp. Mobile Ad Hoc Networking and Computing,* pp. 80-91, Oct. 2002.

[11] C. Bettstetter, "On the Connectivity of Ad Hoc Networks," *The Computer J.,* vol. 47, no. 4, pp. 432-447, 2004.

[12] C. Àlvarez, J. Díaz, J. Petit, J. Rolim, and M. Serna, "High Level Communication Functionalities for Wireless Sensor Networks," *Theoretical Computer Science,* vol. 406, no. 3, pp. 240-247, Oct. 2008.

[13] P. Santi and D. Blough, "The Critical Transmitting Range for Connectivity in Sparse Wireless Ad Hoc Networks," *IEEE Trans. Mobile Computing,* vol. 2, no. 1, pp. 25-39, Jan.-Mar. 2003.

[14] L. Kleinrock and J. Silvester, "Optimum Transmission Radii for Packet Radio Networks or Why Six Is a Magic Number," *Proc. IEEE Nat'l Telecomm. Conf.,* Dec. 1978.

[15] H. Takagi and L. Kleinrock, "Optimal Transmission Ranges for Randomly Distributed Packet Radio Terminals," *IEEE Trans. Comm.,* vol. COM-32, no. 3, pp. 246-257, Mar. 1984.

[16] F. Xue and P.R. Kumar, "The Number of Neighbors Needed for Connectivity of Wireless Networks," *Wireless Networks,* vol. 10, no. 2, pp. 169-181, Oct. 2004.

[17] S. Song, D.L. Goeckel, and D. Towsley, "An Improved Lower Bound to the Number of Neighbors Required for the Asymptotic Connectivity of Ad Hoc Networks," *IEEE Trans. Information Theory,* 2005.

[18] M.D. Penrose, "On K-Connectivity for a Geometric Random Graph," *Wiley Random Structures and Algorithms,* vol 15, no. 2, pp. 45-164, 1999.

[19] C. Bettstetter, "Connectivity of Wireless Multihop Networks in a Shadow Fading Environment," *Proc. Sixth ACM Int'l Workshop Modeling Analysis and Simulation of Wireless and Mobile Systems,* Sept. 2003.

[20] D. Kundur, W. Luh, U.N. Okorafor, and T. Zourntos, "Security and Privacy for Distributed Multimedia Sensor Networks," *Proc. IEEE,* special issue on recent advances in distributed multimedia comm., vol. 96, no. 1, pp. 112-130, Jan. 2008.

[21] D. Kundur and U.N. Okorafor, "A Secure Integrated Routing and Localization Scheme for Broadband Mission Critical Networks," *Proc. IEEE INFOCOM Workshop Mission Critical Networks,* pp. 1-6, Apr. 2008.

[22] *Introduction to the Theory of Coverage Processes,* P. Hall, ed. John Wiley & Sons, 1988.

[23] *Statistics for Spatial Data,* N. Cressie, ed. John Wiley & Sons, 1991.

[24] S. Trisno, "Design and Analysis of Advanced Free Space Optical Communication Systems," PhD dissertation, Dept. of Electrical and Computer Eng., Univ. of Maryland, June 2006.

[25] T. Ernst and W. Dabbous, "A Circuit-Based Approach for Routing in Unidirectional Links Networks," INRIA Research Report RR-3292, Nov. 1997.

[26] J.M. Kahn, R.H. Katz, and K.S.J. Pister, "Next Century Challenges: Mobile Networking for 'Smart Dust'," *Proc. ACM/IEEE Int'l Conf. Mobile Computing and Networking,* pp. 271-278, Aug. 1999.

[27] S. Bandyopadhyay and E.J. Coyle, "An Energy Efficient Hierarchical Clustering Algorithm for Wireless Sensor Networks," *Proc. IEEE INFOCOM,* 2003.

[28] B. Liu and D. Towsley, "A Study of the Coverage of Large-Scale Sensor Networks," *Proc. First IEEE Int'l Conf. Mobile Ad-Hoc and Sensor Systems,* Oct. 2004.

[29] *The Design and Analysis of Computer Algorithms,* A.V. Aho, J.E. Hopcroft, and J.D. Ullman, eds. Addison-Wesley, 1974.

[30] *Introduction to Algorithms,* T. Cormen, C.E. Leiserson, R.L. Rivest, and C. Stein, eds., second ed. MIT press, 2001.
[31] A. Amis and R. Prakash, "Load-Balancing Clusters in Wireless Ad Hoc Networks," *Proc. Third IEEE Symp. Application-Specific Systems and Software Eng. Technology,* pp. 25-32, Mar. 2000.
[32] B. Das and V. Bharghavan, "Routing in Ad-Hoc Networks Using Minimum Connected Dominating Sets," *Proc. IEEE Int'l Conf. Comm. (ICC '97),* vol. 1, pp. 376-380, June 1997.
[33] W. Heinzelman, A. Chandrakasan, and H. Balakrishnan, "Energy-Efficient Communication Protocols for Wireless Microsensor Networks," *Proc. Hawaiian Int'l Conf. Systems Science,* Jan. 2000.
[34] O. Younis and S. Fahmy, "Distributed Clustering in Ad-Hoc Sensor Networks: A Hybrid, Energy-Efficient Approach," *Proc. IEEE INFOCOM,* 2004.
[35] J. Díaz, D. Mitsche, and X. Perez, "Dynamic Random Geometric Graphs," *Discrete Math.,* Apr. 2007.

Unoma Ndili Okorafor received the BSc degree in electrical and computer engineering from the University of Lagos, Nigeria, in 1998, the MSc degree in electrical and computer engineering from Rice University, Houston, Texas, in 2001, and the PhD degree in electrical and computer engineering at Texas A&M University in 2008. Her research interests include secure authentication, secure routing, privacy, and connectivity analysis for WIFI and directional, broadband wireless sensor networks. She currently works as a software engineer with Texas Instruments Education Technology Division in Dallas. In the summer of 2008, she was a visiting professor at the African University of Science and Technology in Abuja, Nigeria. She has been a recipient of the Sloan Foundation Fellowship, the AAUW Engineering Dissertation Fellowship, the US National Science Foundation Fellowship for enhancing STEM education in middle schools, and the Schlumberger Faculty for the Future Fellowship. She is a member of the IEEE, SPIE, NSBE, and SWE.

Deepa Kundur received the BASc, MASc, and PhD degrees in electrical and computer engineering from the University of Toronto, Canada, in 1993, 1995, and 1999, respectively. In January 2003, she joined the Department of Electrical Engineering at Texas A&M University, College Station, where she holds the position of associate professor. Her research interests include protection of scalar and broadband sensor networks, multimedia security, and computer forensics. She is an elected member of the IEEE Information Forensics and Security Technical Committee, the vice chair of the Security Interest Group of the IEEE Multimedia Communications Technical Committee, and is on the editorial boards of *IEEE Communication Letters*, the *IEEE Transactions on Multimedia*, and the *EURASIP Journal on Information Security*. She was recently the general chair for the 2007 ACM Workshop on Multimedia and Security and a guest editor for the 2007 *EURASIP Journal on Advances in Signal Processing* special issue on visual sensor networks. She was a guest editor for the 2004 *Proceedings of the IEEE* special issue on enabling security technologies for digital rights management and the recipient of the 2005 Tenneco Meritorious Teaching Award, the 2006 Association of Former Students College Level Teaching Award, and the 2007 Outstanding Professor Award in the ECE Department at Texas A&M University. She is a senior member of the IEEE.